PHYSICAL REVIEW B VOLUME 39, NUMBER 14 15 MAY 1989-I

Stress-induced splitting of the vibrational absorption of the CN^- ion in alkali halide crystals

G. K. Pandey,* M. Massey, K. L. Pandey, and Raj Kumar
Department of Physics, Allahabad University, Allahabad 211 002, Uttar Pradesh, India
(Received 31 August 1988)

Within the framework of a two-parameter octahedral potential for a dipolar impurity in ionic crystals, it is possible for the impurity to possess minimum-energy orientational configurations in two crystallographic directions simultaneously. Two possible combinations are ⟨111⟩-⟨110⟩ and ⟨111⟩-⟨100⟩. Theory for the effect of stress on tunneling levels for these two models has been developed in this paper and an attempt has been made to explain the tunneling structures in the vibrational absorption of a CN^- impurity ion in KCl, KBr, KI, and RbCl crystals on the basis of these models without incorporating the soft aspects.

I. INTRODUCTION

Orientational tunneling motions of defects in solids have received considerable attention in the past few years. A number of experiments have been performed on such systems as Li^+, OH^-, and CN^- in alkali halide crystals. For a comprehensive review and extensive references one can see the review article by Narayanamurti and Pohl.[1] Most of the qualitative features of these experiments were interpreted in terms of either the Devonshire model,[2] or the pocket-state model as proposed by Gomez, Bowen, and Krumhansl,[3] by Shore,[4] and by Pfister.[5] Recently careful experiments on some of the systems like NaBr:F^-,[6–8] KBr:Li^+,[9,10] KI:OH^-,[11] KCl:CN^-,[12] etc., revealed that certain experimental results are still contradictory or controversial.[12,13] This demanded more accurate experiments with greater accuracy and intuition and the same have been recently reported in the literature (at least for some of the systems). To be specific, Luty[12,14] tried to see the tunneling structure in the vibrational absorption of OH^- and CN^- in KCl. Keeping in mind the small value of the tunneling parameters for these systems, he studied the effect of the applied electric field (on the former) and the applied stress field (on the latter), particularly for increasing the splitting of the vibrational levels. For the latter system, namely, KCl:CN^-, Luty could at best observe characteristic anisotropic changes of the spectral shape. The vibrational absorptions were broadened. The observed second-moment absorption changes (due to quantum-mechanical mixing of the tunneling states by the applied stress) and zero moment changes (due to classical elastic dipole alignment) for the different stress directions confirmed the ⟨111⟩ equilibrium orientation for the defect in the KCl:CN^- system.

More recently, Beyeler,[13] using an infrared grating spectrometer with a maximal resolution power at 5 μm (the wavelength of the vibrational absorption of CN^-), could resolve the tunneling structure and its changes under stress in full detail. In addition paraelastic sidebands were for the first time observed and studied up to the highest achievable paraelastic splittings. Thus Beyeler presented a great amount of spectroscopic data on the CN^- alkali halide systems. Beyeler[13] and also Luty[12] claim (and as it appears quite rightly) that their data conclusively confirm the ⟨111⟩ orientational configuration, contrary to the formerly accepted ⟨100⟩ tunneling model for these systems.[1] However, the detailed quantitative analysis reveals that certain soft aspects have to be introduced to the rigid tunneling model.[13] The two important soft aspects discussed are (a) appreciable changes to the tunneling matrix elements and (b) deviations of equilibrium orientations from the ⟨111⟩ axis under applied stress. The largest change in the nearest-neighbor tunneling matrix element was to be incorporated for the KCl:CN^- system.

Beyeler has assumed that the softness is an inherent property of systems with a large tunneling splitting and hence, a relatively weak hindered rotation potential. There is, however, the KCl:Li^+ system, also a ⟨111⟩ oriented tunneling defect system, with a nearest-neighbor tunneling matrix element comparable to CN^- in KCl ($\eta=0.55$ cm^{-1}) in which no appreciable changes of the tunneling matrix element under uniaxial stress have been observed.[15,16]

Recently, we[17] have shown that, within the framework of a two-parameter octahedral potential, it is possible for the impurity to possess two orientational configurations simultaneously. In the K-K' plot (see Fig. 1 of Ref. 17), we have divided areas in which this kind of situation could occur. We have also hinted that where the parameters K and K' are such that they do not fall in the doubly shaded regions of the K-K' plot, one has potential minima along one crystallographic direction only. This is, perhaps, the case for the system like KCl-Li^+.[18–21]

The second situation is one in which the values of K and K' do fall in the doubly shaded region, so that one has simultaneous potential minima along two crystallographic directions. But in this limit also, one well could be deeper than the other. In such cases, if the upper well is not populated enough at a given temperature, the system again behaves like an ideal paraelectric system with potential minima effectively along one crystallographic direction only.

The third interesting situation is one in which both the wells are almost equally deep. Under such cir-

cumstances, the behavior of the system becomes crucial to the experimental conditions and one gets controversial results in different experimental circumstances.

In the present paper we wish to examine whether the experimental results of Beyeler can be interpreted in terms of the model of potential minima along the two crystallographic directions, without incorporating the soft aspects. In view of the strong experimental evidence that CN^- aligns along either of the eight $\langle 111 \rangle$ directions, we assume that the second situation (as mentioned above) applies to these systems. That is, the $\langle 111 \rangle$ wells are deeper. The upper wells could be either along the twelve $\langle 110 \rangle$ or the six $\langle 100 \rangle$ directions, depending upon the relative values of K and K'. In the following sections, we first build up the theory for the effect of uniaxial stress (along different crystallographic directions) on the two potential minima model. This is done for both the situations, viz., simultaneous occurrence of $\langle 111 \rangle$ and $\langle 110 \rangle$ wells and that of $\langle 111 \rangle$ and $\langle 100 \rangle$ wells. We then examine the relative merits of the two models in explaining the experimental results on the systems considered and discuss the results accordingly.

II. THEORY

The total Hamiltonian for the system with applied uniaxial stress can be written as

$$H = H_t + H_s \ ,$$

where H_t is the tunneling Hamiltonian, which has off-diagonal elements $-\eta$ connecting the nearest neighboring wells of the eight $\langle 111 \rangle$ states, off-diagonal elements $-\eta'$ connecting the nearest neighboring wells of the twelve $\langle 110 \rangle$ states, and $-\chi$ connecting a state of the eight $\langle 111 \rangle$ wells to one of the nearest neighboring wells of the twelve $\langle 110 \rangle$ states. (See Appendix A of Ref. 17.)

The stress Hamiltonian can be written as

$$H_s = \sum_{\mu,\nu} h_\mu(\Gamma^\nu) e_\mu(\Gamma^\nu) \ .$$

The factors $h_\mu(\Gamma^\nu)$ are linear combinations of the first derivatives of the potential coupling the model to the host lattice. These are tabulated in Appendix IV of the paper by Gomez *et al.*[3] If α, β, and γ are the direction cosines of the uniaxial stress $-P_{lk}$ with respect to the cube's principal axes, then the factors $e_\mu(\Gamma^\nu)$ may be written as

$$e(A_{1g}) = -(S_{11}+2S_{12})P \ ,$$

$$e_1(E_g) = -(2\gamma^2-\alpha^2-\beta^2)(S_{11}-S_{12})P \ ,$$

$$e_2(E_g) = -(\alpha^2-\beta^2)(S_{11}-S_{12})P \ ,$$

TABLE I. The diagonal elements of H_s for case I, i.e., the case of simultaneous potential minima along the $\langle 111 \rangle$ and $\langle 110 \rangle$ directions. [For the designation of the potential wells, see Fig. 1(a) of Ref. 17.]

(i) For the eight $\langle 111 \rangle$ wells

$H_s(a,a) = \xi(\alpha\beta+\beta\gamma+\gamma\alpha)$
$H_s(b,b) = -\xi(\alpha\beta-\beta\gamma+\gamma\alpha)$
$H_s(c,c) = -\xi(-\alpha\beta+\beta\gamma+\gamma\alpha)$
$H_s(d,d) = -\xi(\alpha\beta+\beta\gamma-\gamma\alpha)$
$H_s(e,e) = -\xi(-\alpha\beta+\beta\gamma+\gamma\alpha)$
$H_s(f,f) = -\xi(\alpha\beta+\beta\gamma-\gamma\alpha)$
$H_s(g,g) = \xi(\alpha\beta+\beta\gamma+\gamma\alpha)$
$H_s(h,h) = -\xi(\alpha\beta-\beta\gamma+\gamma\alpha)$

(ii) For the twelve $\langle 110 \rangle$ wells

$H_s(A,A) = \xi'(\alpha^2+\beta^2-2\gamma^2)/3+\xi\alpha\beta$
$H_s(B,B) = \xi'(\alpha^2+\beta^2-2\gamma^2)/3-\xi\alpha\beta$
$H_s(C,C) = \xi'(\alpha^2+\beta^2-2\gamma^2)/3+\xi\alpha\beta$
$H_s(D,D) = \xi'(\alpha^2+\beta^2-2\gamma^2)/3-\xi\alpha\beta$
$H_s(E,E) = \xi'(\alpha^2-2\beta^2+\gamma^2)/3-\xi\alpha\gamma$
$H_s(F,F) = \xi'(\alpha^2-2\beta^2+\gamma^2)/3+\xi\alpha\gamma$
$H_s(G,G) = \xi'(\alpha^2-2\beta^2+\gamma^2)/3-\xi\alpha\gamma$
$H_s(H,H) = \xi'(\alpha^2-2\beta^2+\gamma^2)/3+\xi\alpha\gamma$
$H_s(K,K) = \xi'(-2\alpha^2+\beta^2+\gamma^2)/3-\xi\beta\gamma$
$H_s(L,L) = \xi'(-2\alpha^2+\beta^2+\gamma^2)/3+\xi\beta\gamma$
$H_s(M,M) = \xi'(-2\alpha^2+\beta^2+\gamma^2)/3-\xi\beta\gamma$
$H_s(N,N) = \xi'(-2\alpha^2+\beta^2+\gamma^2)/3+\xi\beta\gamma$

$$e_1(T_{2g}) = -S_{44}\beta\gamma P \ ,$$

$$e_2(T_{2g}) = -S_{44}\alpha\gamma P \ ,$$

$$e_3(T_{2g}) = -S_{44}\alpha\beta P \ .$$

Here, $-P$ is the magnitude of the stress, e.g., $-P_{lk} = -\alpha\beta P$, and S_{11}, S_{12}, and S_{44} are the elastic stiffness constants of the lattice adjacent to the impurity.

Leaving the symmetric and angle-independent part, which causes equal shifts to all the levels, we get H_s as

TABLE II. The diagonal elements of H_s for case II, i.e., the case of simultaneous potential minima along the $\langle 111 \rangle$ and $\langle 100 \rangle$ directions.

(i) For the eight $\langle 111 \rangle$ wells

Same as given in Table I

(ii) For the six $\langle 100 \rangle$ wells

$H_s(A,A) = \xi'(4\alpha^2-2\beta^2-2\gamma^2)$
$H_s(B,B) = \xi'(-2\alpha^2+4\beta^2-2\gamma^2)$
$H_s(C,C) = \xi'(4\alpha^2-2\beta^2-2\gamma^2)$
$H_s(D,D) = \xi'(-2\alpha^2+4\beta^2-2\gamma^2)$
$H_s(E,E) = \xi'(-2\alpha^2-2\beta^2+4\gamma^2)$
$H_s(F,F) = \xi'(-2\alpha^2-2\beta^2+4\gamma^2)$

$$H_s = Px\frac{\partial V}{\partial x}\left[\frac{2\gamma^2-4\alpha^2+2\beta^2}{6}(S_{11}-S_{12})\right]+Py\frac{\partial V}{\partial y}\left[\frac{2\gamma^2+2\alpha^2-4\beta^2}{6}(S_{11}-S_{12})\right]$$

$$+Pz\frac{\partial V}{\partial z}\left[\frac{-4\gamma^2+2\alpha^2+2\beta^2}{6}(S_{11}-S_{12})\right]+P\left[x\frac{\partial V}{\partial y}+y\frac{\partial V}{\partial x}\right]\left[\frac{-\alpha\beta}{2}S_{44}\right]$$

$$+P\left[y\frac{\partial V}{\partial z}+z\frac{\partial V}{\partial y}\right]\left[-\frac{\beta\gamma}{2}S_{44}\right]+P\left[z\frac{\partial V}{\partial x}+x\frac{\partial V}{\partial z}\right]\left[-\frac{\gamma\alpha}{2}S_{44}\right].$$

With the above formulation, the stress Hamiltonian for the two cases, viz., the ⟨111⟩-⟨110⟩ model and the ⟨111⟩-⟨100⟩ model, can be written in the matrix form and are summarized in Tables I and II. Here, the stress Hamiltonian is in the pocket-state representation and has only diagonal terms. Further, we have defined

$$\xi = -Px\frac{\partial V}{\partial y}S_{44} = -\alpha_1 P\ ,$$

$$\xi' = -Px\frac{\partial V}{\partial y}(S_{11}-S_{12}) = -\alpha_2 P\ .$$

α_1 and α_2 are the paraelastic splitting factors. When the wave functions are expressed according to the irreducible representation of the O_h point group, the total Hamiltonian is transformed to $H' = U^{\dagger}HU$, where U is the proper transformation matrix, transforming the pocket states to the irreducible representation states of the O_h point group. For the stress directions ⟨111⟩, ⟨110⟩, and ⟨001⟩ for which experimental data are available, H' is diagonalized in each case to get the energy eigenvalues, eigenfunctions, transition frequencies, and transition strengths.

III. RESULTS AND DISCUSSION

Our main emphasis will be on CN^- impurity in alkali halide crystals, as has recently been investigated by Luty[12] and Beyeler.[13] Both these workers considered a rigid ⟨111⟩ tunneling model. For this model, the splitting of the ground and first excited vibrational levels due to tunneling and due to stress along the ⟨111⟩, ⟨110⟩, and ⟨001⟩ directions has been worked out by Gomez *et al.* and is summarized here in Fig. 1 for ready reference. In Figs. 2 and 3 we present the same thing for the two models considered in this work, viz., a model of simultaneous occurrence of potential minima along the ⟨111⟩ and ⟨110⟩ crystallographic directions and that of simultaneous occurrence of potential minima along the ⟨111⟩ and ⟨100⟩ directions. For both of these models, it is assumed that the ⟨111⟩ wells are deeper and that the center of the ⟨110⟩ and ⟨100⟩ multiplets lies at a higher energy p above it. At low temperatures (LHT) at which the experiments of Luty and Beyeler have been performed, one can fairly well assume that only the lower ⟨111⟩ levels will be well enough populated. Hence the entire experimental results should be explainable with the lower ⟨111⟩ energy levels only. In Figs. 2 and 3, we therefore depict only these levels. It may be mentioned that above an energy p from the center of the ⟨111⟩ levels, multiplets corresponding to ⟨110⟩ or ⟨100⟩ wells will also be presented and they also split and change with the applied uniaxial stress. Thus our attempt to explain the results will primarily be based on the effect of the second set of potential minima on the energy level structure of the lower ⟨111⟩ states and its variations under uniaxial stress applied along different crystallographic directions. A preliminary check on the relative merits of the two models shows that the experimental results obtained for stress field effect on the systems under consideration cannot be explained on the basis of the ⟨111⟩-⟨100⟩ model. Firstly, under ⟨111⟩ stress, the levels A_{1g} and A_{2u} cross each other [Fig. 3(b)]. But this effect is not observed experimentally. Secondly, this model predicts no effect of ⟨001⟩ stress on the ⟨111⟩ tunneling levels [Fig. 3(d)], while Beyeler has observed quite noticeable spectral changes under ⟨001⟩ stress. As such, we reject the ⟨111⟩-⟨100⟩ model for the present systems, and in the following subsections, the experimental results are compared with the theoretical predictions of the ⟨111⟩-⟨110⟩ model, with due emphasis on the KCl:CN^- system. The other systems, viz., KBr:CN^-, KI:CN^-, and RbCl:CN^- show similar results and, where necessary, these systems are also included in the discussions.

A. CN^- in KCl

1. *Analysis of the zero-field structure*

The ⟨111⟩model gives three zero-field tunneling transitions of the same frequency if we consider only the nearest-neighbor tunneling [Fig. 1(a)]. The separation between Stokes-anti-Stokes vibrational absorption is equal to four times the nearest-neighbor tunneling matrix element η. Experimentally, $|\eta| = 0.63\ \text{cm}^{-1}$. The observed linewidth of $0.3\ \text{cm}^{-1}$ in the two lines[13] places an upper limit on the value of the next-nearest-neighbor tunneling matrix element μ: $|\mu| \leq 0.04\ \text{cm}^{-1}$.

The theoretical predictions of the ⟨111⟩-⟨110⟩ and ⟨111⟩-⟨100⟩ models give different frequencies for the three transitions [Figs. 2(a) and 3(a)]. In the context of the ⟨111⟩-⟨110⟩ model, Fig. 2(a) shows that for a finite value of χ, the three stress transitions become unequal. This effect becomes pronounced with larger χ and smaller p values. One finds that the A_{2u}-T_{2g} transition occurs at a slightly higher frequency, while the other two transitions, viz., T_{2g}-T_{1u} and T_{1u}-A_{1g} occur at almost equal but lower to the A_{2u}-T_{2g} transition frequency. Thus, ac-

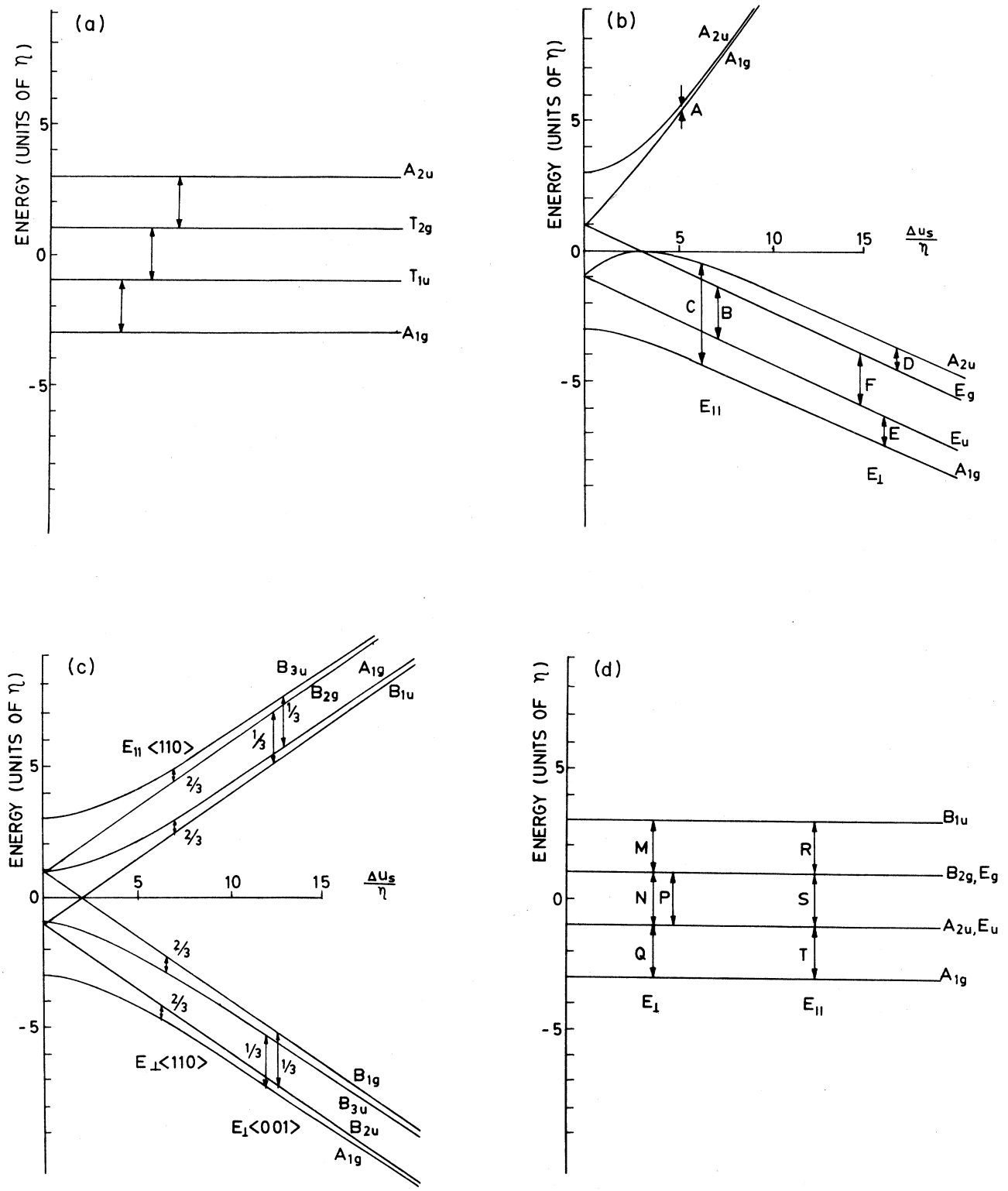

FIG. 1. (a) Energy level structure for the ⟨111⟩ off-centered impurity when nearest-neighbor tunneling parameter η is dominant. A_{1g}, T_{1u}, T_{2g}, and A_{2u} are the irreducible representation of the O_h group. (b) Stress field splittings for the ⟨111⟩ off-centered impurity system, when η is the dominant tunneling parameter with the corresponding allowed dipolar transitions for the E vector of the e.m. radiation parallel and perpendicular to the stress direction. (b) For stress along the ⟨100⟩ direction, (c) for stress along the ⟨110⟩ direction, and (d) for stress along the ⟨111⟩ direction.

cording to the ⟨111⟩-⟨110⟩ model, the zero-field absorption should have doublet structure in Stokes and anti-Stokes lines. Figures 4, 6, and 18 of Ref. 13 show that the doublet structure is indeed observed for the anti-Stokes line appearing at the lower frequency, but the same is not observed for the Stokes line. The doublet structure in the anti-Stokes absorption is real and has been admitted in Ref. 13. The reason for the nonappearance of the doublet structure in the Stokes line is not very clear to us and at the present moment we are not in a position to comment on that. Beyeler's contention on this is the possible coupling between the vibrational and tunnel-

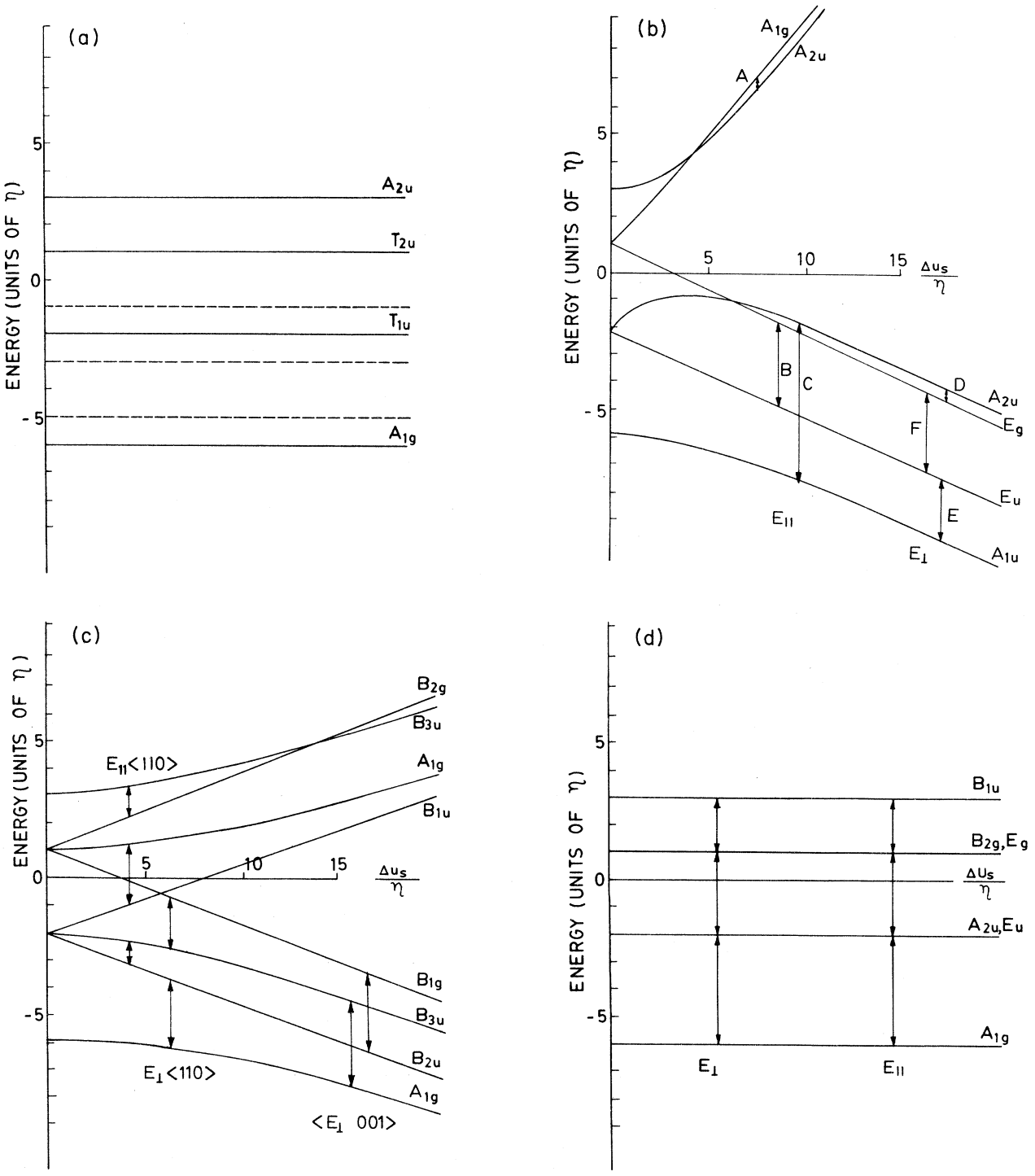

FIG. 2. (a)–(d) Same as in Fig. 1 but for the case of simultaneous occurrence of potential minima along the ⟨111⟩ and ⟨100⟩ directions.

ing states of the impurity. However, within the Born-Oppenheimer approximation, this seems to be unlikely. (The vibrational energy states of the impurity are 3 orders of magnitude larger than the tunneling energy.)

The reported splitting by about 0.2 cm^{-1} in the anti-Stokes line with Stokes and anti-Stokes lines at ± 1.26 cm^{-1} is obtained from the $\langle 111 \rangle$-$\langle 110 \rangle$ model by taking the following parameters: $\eta=0.63$, $\eta'=0.03$, $\chi=1.53$, and $p=11.33$ cm^{-1}, and the stress coupling factors $\alpha_1=12.5\times10^{-24}$ cm and $\alpha_2=7.5\times10^{-24}$ cm^3. We shall discuss the effect of uniaxial stress in different directions with the same set of parameters.

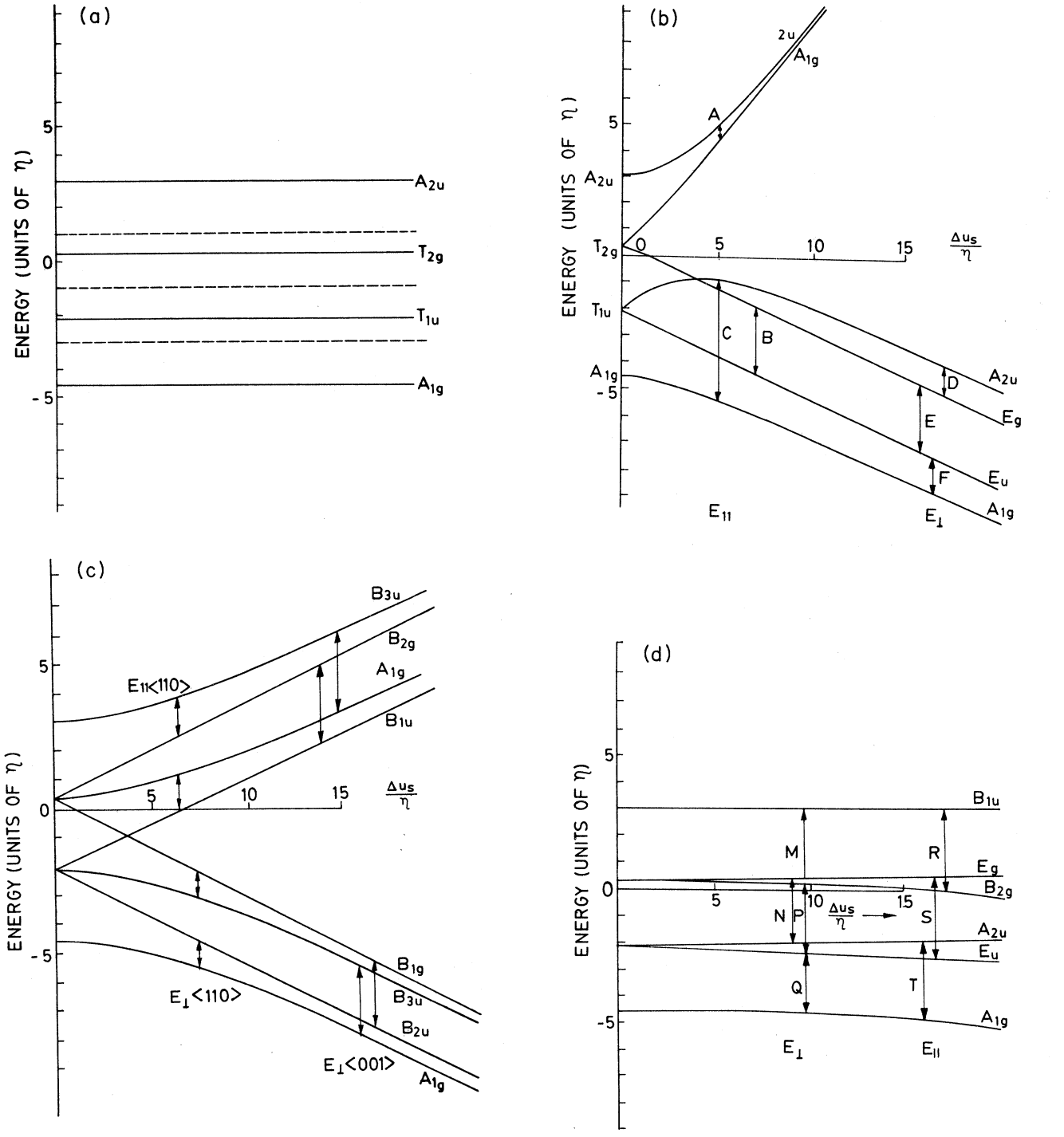

FIG. 3. (a)–(d) Same as in Fig. 1 but for the case of simultaneous occurrence of potential minima along the $\langle 111 \rangle$ and $\langle 110 \rangle$ directions.

2. *Effects of ⟨111⟩ stress*

The rigid ⟨111⟩ dipole model suggests that under ⟨111⟩ stress with $E_{\parallel}$, three transitions [labeled as *A*, *B*, and *C* in Fig. 1(b)] are possible. The *B* transition is all along independent of stress, while transitions *A* and *C* are stress dependent for small stresses, but they too become stress independent for large stress. Qualitatively, three such transitions are indeed observed [see Fig. 4 of Ref. 13]. This fact positively establishes the levels involved for these observations belong to the ⟨111⟩ oriented defect system. Similarly, under ⟨111⟩ stress and $E_{\perp}$, the rigid ⟨111⟩ tunneling model again predicts three transitions labeled as *D*, *E*, and *F* in Fig. 1(b). Even this is in qualitative agreement with the observations of Beyeler. However, when the results are quantitatively compared, certain discrepancies become obvious. The prominent one is for $E_{\parallel}$. Beyeler observed that the *B* transition does not at all remain stress independent, but its frequency increases linearly with stress. Similarly, the transition frequency of *C* transition does not attain stress-independent value at large stresses, but goes on increasing linearly. Similar discrepancies are also observed for the $E_{\perp}$ case. These observations are summarized in Figs. 4(a) and 4(b). The solid line represents the predictions of the rigid ⟨111⟩ model, whereas the experimental results are illustrated by solid circles.

Beyeler tried to explain the results empirically by postulating that the tunneling splitting parameter η becomes stress dependent. This dependence can be calculated by plotting the *B* transition frequency divided by 2 as a function of stress. The result has been presented in Fig. 9 of Ref. 12 and has also been presented here in Fig. 5 for ready reference.

The theoretical predictions of the model of simultaneous occurrence of potential minima along the ⟨111⟩ and ⟨110⟩ directions will now be discussed. Figure 2(b) shows the result of ⟨111⟩ stress on the ⟨111⟩-⟨110⟩ model energy levels for the set of parameters η, η', etc. as given above. Qualitatively, Fig. 2(b) does not seem to differ much from Fig. 1(b), but the difference is there and becomes more visible, when the results are plotted in Figs. 4 and 5. The dashed lines in Figs. 4(a) and 4(b) show the calculated results as expected from this model. Similarly, in Fig. 5, the dashed line shows the variation of the *B* transition frequency divided by 2 as a function of stress. From the comparisons in Figs. 4(a), 4(b), and 4(c) it becomes apparent that the experimental results of Beyeler can also be understood in terms of the model of simultaneous occurrence of potential minima along the ⟨111⟩ and ⟨110⟩ directions. This may avoid the need to introduce the so-called "soft aspects" in the tunneling model.

3. *Effect of ⟨110⟩ stress*

The spectral changes under ⟨110⟩ stress show similar features for the *E* parallel and perpendicular cases. Here the doublet structure narrows down and at high stress gets converted into a single line. For $E_{\perp}$, the doublet structure is retained to the highest applied stress. These

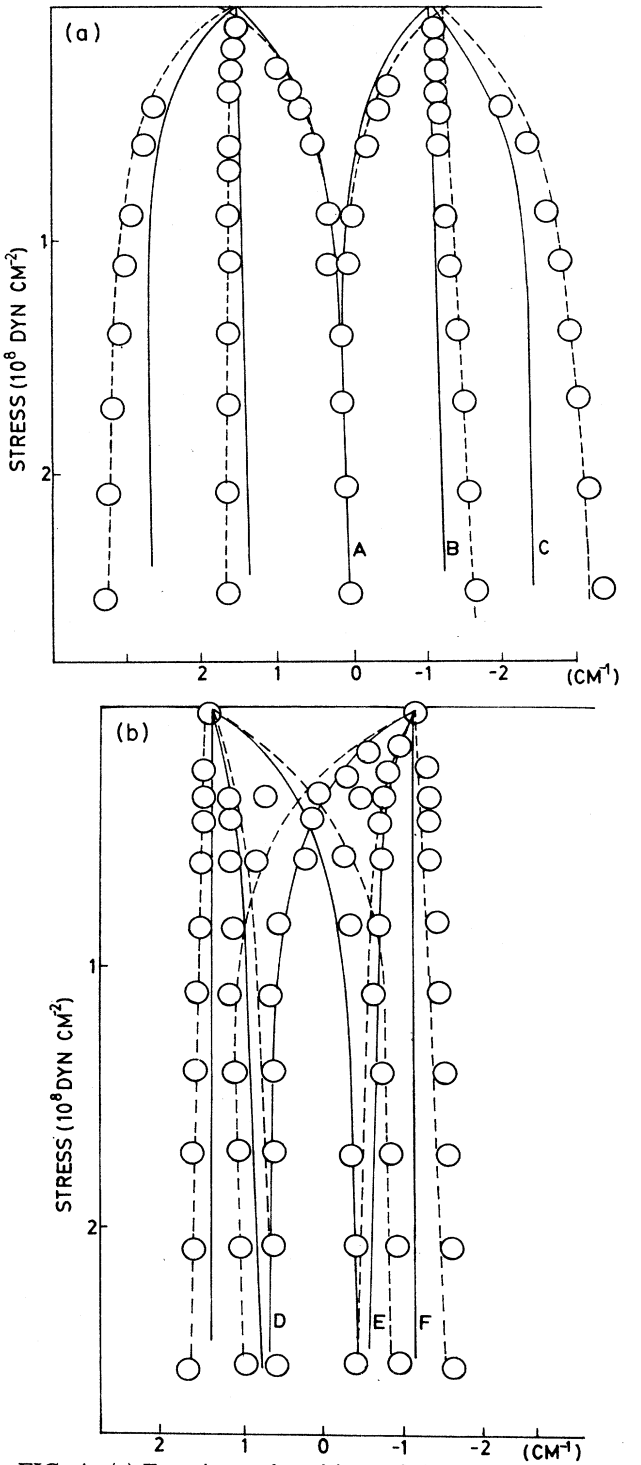

FIG. 4. (a) Experimental positions of the observed lines for KCl:CN$^-$ under ⟨111⟩ stress for the case when the *E* vector of the e.m. radiation is parallel to the stress direction (○–○–○). The solid line represents the expected behavior for the rigid ⟨111⟩ tunneling model, the dashed line (— — —) represents the expected behavior for the model of simultaneous occurrence of potential minima along the ⟨111⟩ and ⟨110⟩ directions with the parameters η, η', χ, and p as reported in the text. (b) Same as in (a) but for the case when the *E* vector of the e.m. radiation is perpendicular to the stress direction.

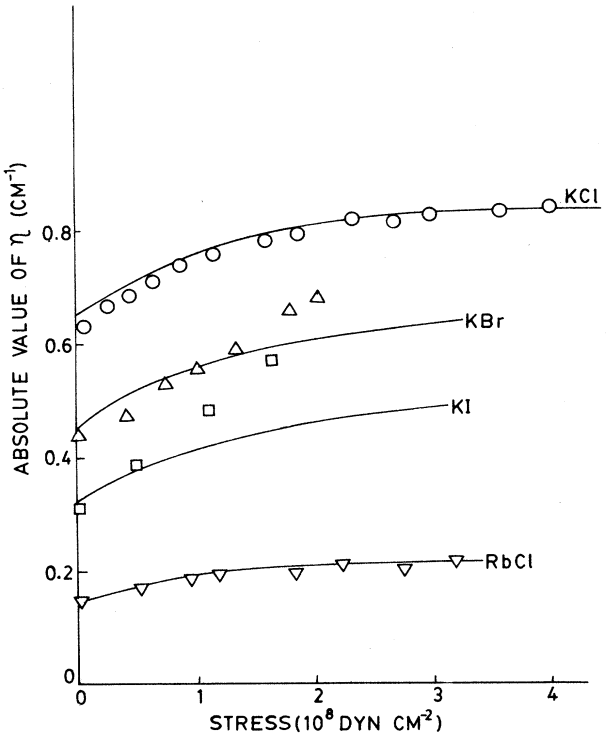

FIG. 5. Stress dependence of η empirically calculated by Beyeler as the B transition frequency divided by 2. The solid line represents the B transition frequency divided by 2 based upon the calculations of simultaneous occurrence of the ⟨111⟩ and ⟨110⟩ potential wells, without incorporating the soft aspects.

features are well explained by both the ⟨111⟩ rigid tunneling model [Fig. 1(c)] and the ⟨111⟩-⟨110⟩ model [Fig. 2(c)]. While the ⟨111⟩ model gives a rapid rate of decrease of the separation between the doublet structure for $E_{\parallel}$ and $E_{\perp}$, the ⟨111⟩-⟨110⟩ model gives a slower rate of decrease. The predictions of the ⟨111⟩-⟨110⟩ model have better agreement with the experimental results of Beyeler.

For $E_{\perp}$, Beyeler has reported that two lines appearing from the doublet structure move rapidly towards the center and are lost in the central line at very low stress values. None of the models discussed so far is able to account for these lines.

4. *Effect of ⟨100⟩ stress*

The energy level structure for the rigid ⟨111⟩ model under ⟨100⟩ stress is shown in Fig. 1(a). One can readily see that the level structure is independent of the applied stress. Hence, according to this model, no stress-induced effect should be observed. However, Beyeler has observed noticeable spectral changes under ⟨100⟩ stress. The doublet structure is preserved in both polarizations, but for $E_{\parallel}$ the splitting increases with the stress and reaches 8 cm^{-1} for highest achieved stress. For $E_{\perp}$ the splitting decreases sizably. The ⟨111⟩-⟨110⟩ model accounts for these features well as shown in Figs. 4(d) and 6.

B. CN^- in KBr and KI

For the KBr:CN^- and KI:CN^-, the rate of variation of η with stress is quite large. For fitting this type of be-

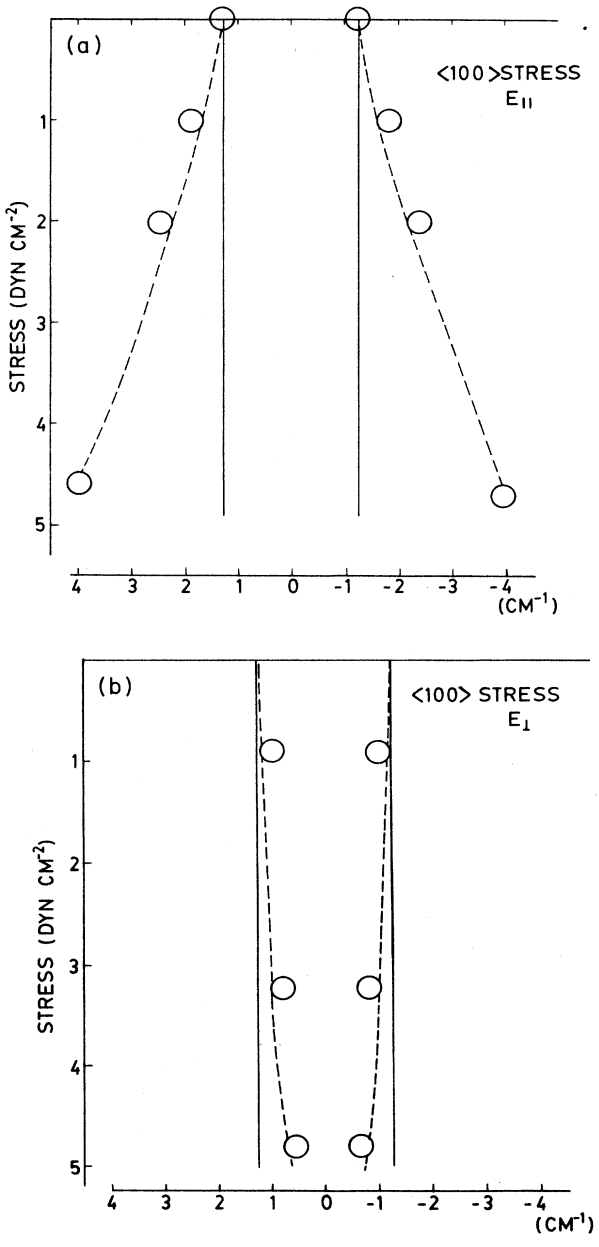

FIG. 6. Stress dependence under ⟨100⟩ stress. The solid line represents the predictions of the rigid ⟨111⟩ model. Circles represent the experimental observations of Beyeler (extrapolated from Fig. 6 of Ref. 18). The dashed line represents the calculated behavior according to the model considered in this work (see text).

havior in terms of the present model, one has to use large χ and relatively small p values. With small p values, the upper multiplet of energy states, due to the 12 ⟨110⟩ wells should also be considered, because at some value of stress, some of the energy states of the lower ⟨111⟩ multiplet come near some of those of the upper ⟨110⟩ multiplet. At this value of stress, level turning takes place, and a behavior similar to that observed with the electric field effects in KI:OH^- is seen. Thus the model predicts some sort of backward lines and nonlinearity at high stress values. The exact value of the stress at which this turning of levels takes place depends mostly on the value of p. Also, the transition frequency at the turning point depends mostly on the value of χ. For large p, this kind of behavior is expected at very high stress values, which in most of the cases becomes unattainable due to experimental difficulties. The experimental data available for the KBr:CN^- and KI:CN^- are not enough to pursue the application of our model on these systems any further at the present.

C. CN^- in RbCl

The effect of ⟨111⟩ stress on the RbCl system shows effects similar to that for the KCl:CN^- system and the stress dependence of the B and C transitions is very well explained by the ⟨111⟩-⟨110⟩ model (Fig. 5) for $\eta=0.15$ cm^{-1}, $\eta'=0.03$ cm^{-1}, $\chi=1.0$ cm^{-1}, $p=5.2$ cm^{-1}, $\alpha_1=8.0\times10^{-24}$ cm^3, and $\alpha_2=6.3\times10^{-24}$ cm^3.

IV. SUMMARY AND CONCLUSIONS

The experimental study of the tunneling transitions in the form of combined vibrational tunneling transitions has shown that the simple ⟨111⟩ tunneling model is able to account for most of the salient features of the spectral variations with stress. But there are some additional features which call for modification of the old model. The two-parameter octahedral potential gives scope for the simultaneous existence of potential minima in two crystallographic directions. The ⟨111⟩-⟨110⟩ model is able to account for most of the experimental features to a remarkable degree, considering the simplicity of the model in which we consider only the nearest-neighbor tunneling. If next-nearest-neighbor tunneling is also taken into account, then better agreement between the experimental results and theoretical predictions is to be expected. Also, the paraelastic splitting factors depend on the potential faced by the impurity in the host matrix and hence should depend upon the off-center displacement of the impurity. If the off-center displacement of the impurity is different in the two wells, then paraelastic splitting factors will be different for the two wells.

Any future theoretical investigation on the basis of the present model should take into consideration the above factors for a better agreement with the experimental results.

ACKNOWLEDGMENTS

The authors are indebted to Dr. V. K. Agrawal for his valuable suggestions and help in computational problems.

*Present address: Department of Physics, Al-Fatah University, P.O. Box 13220, Tripoli, Libya.

[1]V. Narayanamurti and R. O. Pohl, Rev. Mod. Phys. **42**, 201 (1970).
[2]A. F. Devonshire, Proc. R. Soc. London, Ser. A **153**, 601 (1936).
[3]M. Gomez, S. P. Bowen, and J. A. Krumhansl, Phys. Rev. **153**, 1009 (1967).
[4]H. B. Shore, Phys. Rev. **151**, 570 (1966).
[5]G. Pfister, Helv. Phys. Acta **39**, 602 (1966).
[6]R. J. Quigley and T. P. Das, Phys. Rev. B **7**, 4004 (1973).
[7]R. J. Rollefson, Phys. Rev. B **5**, 3235 (1972).
[8]R. J. Rollefson, Phys. Rev. B **7**, 4006 (1973).
[9]A. M. Kahan and A. J. Sievers, Phys. Lett. **37A**, 203 (1971).
[10]R. D. Kirby and A. J. Sievers, Solid State Commun. **6**, 613 (1968).
[11]F. Bridges, Solid State Commun. **13**, 1877 (1973).
[12]F. Luty, Phys. Rev. B **10**, 3667 (1974).
[13]H. U. Beyeler, Phys. Rev. B **11**, 3078 (1975).
[14]A. D. Gangora and F. Luty, Solid State Commun. **14**, 923 (1974).
[15]D. Blumenstock, R. Osswald, and H. C. Wolf, Phys. Status Solidi B **64**, 217 (1971).
[16]T. R. Larson and R. H. Silsbee, Phys. Rev. B **5**, 778 (1972).
[17]G. K. Pandey, K. L. Pandey, M. Massey, and Raj Kumar, Phys. Rev. B **34**, 1277 (1986).
[18]R. J. Russell and F. Bridges, Phys. Rev. B **26**, 3386 (1982).
[19]W. Zollar and F. Bridges, Phys. Rev. B **24**, 4796 (1981).
[20]F. Luty, Phys. Rev. B **25**, 7780 (1982).
[21]W. M. Kelly and F. Bridges, Phys. Rev. B **18**, 4606 (1978).